Monthly Notices
of the
ROYAL ASTRONOMICAL SOCIETY

Mon. Not. R. Astron. Soc. **400,** 422–428 (2009) doi:10.1111/j.1365-2966.2009.15467.x

The role of thermal conduction in magnetized viscous–resistive advection-dominated accretion flows

J. Ghanbari,[1⋆] S. Abbassi[2,3⋆] and M. Ghasemnezhad[1⋆]

[1]*Department of Physics, School of Sciences, Ferdowsi University of Mashhad, Mashhad 91775-1436, Iran*
[2]*School of Physics, Damghan University of Basic Sciences, PO Box 36715-364, Damghan, Iran*
[3]*School of Astronomy, Institute for Research in Fundamental Sciences (IPM), PO Box 19395-5531, Tehran, Iran*

Accepted 2009 July 29. Received 2009 July 29; in original form 2009 March 4

ABSTRACT

Observations of the hot gas that surrounds Sgr A* and a few other nearby galactic nuclei imply that the mean free paths of electrons and protons are comparable to the gas capture radius. Hot accretion flows therefore likely proceed under weak collision conditions. As a result, thermal conduction by ions has a considerable contribution to the transfer of the realized heat in accretion mechanisms. We study a two-dimensional advective accretion disc bathed in the poloidal magnetic field of a central accretor in the presence of thermal conduction. We find self-similar solutions for an axisymmetric, rotating, steady, viscous–resistive, magnetized accretion flow. The dominant mechanism of energy dissipation is assumed to be turbulent viscosity and magnetic diffusivity due to the magnetic field of the central accretor. We show that the global structure of advection-dominated accretion flows (ADAFs) is sensitive to viscosity, advection and thermal conduction parameters. We discuss how the radial flow, angular velocity and density of accretion flows may vary with the advection, thermal conduction and viscous parameters.

Key words: accretion, accretion discs – magnetic fields – MHD.

1 INTRODUCTION

The foundations of our present understanding of advection-dominated accretion flows (ADAFs) were laid out in a series of papers by Narayan & Yi (1994, 1995a,b), although some ideas were anticipated much earlier by Ichimaru (1977). The specific abbreviation ADAF was introduced by Lasota et al. (1996). An ADAF is defined as one in which a large fraction of the viscously generated heat is advected with the accreting gas, and only a small fraction of the energy is radiated. ADAFs have an opposite regime to that of the standard model. In the standard model, the flow is described in such a way that the heat generated by the viscosity radiates out of the system immediately after its generation (Shakura & Sunyaev 1973).

These advection-dominated accretion flows occur in two regimes depending on their mass accretion and optical depth. Actually, the optical depths of accretion flows are highly dependent on their accretion rates. In a high mass-accretion rate, the optical depth becomes very high and the radiation generated by the accretion flow can be trapped within the disc. This type of accretion disc is known as an optically thick or slim disc, terminology that was introduced by Abramowicz et al. (1988). In the limit of low mass-accretion rate, the disc becomes optically thin. In this case, the cooling time of accretion flows is longer than the accreting time-scale. The energy generated by accretion flows therefore remains mostly in the discs, and the discs cannot radiate their energy efficiently. This type of accretion flow is named a radiation-inefficient accretion flow (RIAF). This type of accretion flow has been investigated by many authors (Narayan & Yi 1994; Abramowicz et al. 1995; Chen 1995).

This type of solution has been used to interpret the spectra of X-ray binary black holes in their quiescent or low/hard state as an alternative to the Shapiro, Lightman & Eardley (1976, SLE) solutions. Since ADAFs have large radial velocities and also the infalling matter carries thermal energy to the black hole, the energy transported by advection can stabilize the thermal instability by removing the steep temperature gradient; thus ADAF models have been widely used to explain the observations of low luminosity observed in Sgr A* (Narayan, Maclintock & Yi 1996; Hameury et al. 1997). However, numerical simulations of RIAFs revealed that low-viscosity flows are convectively unstable, and therefore convection strongly influences the global structure of accretion flows (Igumenshchev, Abramowicz & Narayan 2000). Thus, another type of accretion flow was proposed, in which convection plays a dominant role in transporting the energy, angular momentum and locally released viscous energy within the disc.

A notable problem arises when the accretion disc is threaded by a magnetic field. In the ADAF models, the temperature of the accretion disc is so high that the accreting materials are ionized. The

⋆E-mail: ghanbari@ferdowsi.um.ac.ir (JG); sabbassi@dubs.ac.ir (SA); m_ghasemnezhad2005@yahoo.com (MG)

magnetic field therefore plays an important role in the dynamics of accretion flows. Some authors have tried to solve the magnetohydrodynamics (MHD) equations of magnetized ADAFs analytically. For example, Kaburaki (2000) has presented a set of analytical solutions for a fully advective accretion flow in a global magnetic field. Shadmehri (2004) has extended this analysis for a non-constant resistivity. Ghanbari, Salehi & Abbassi (2007) have presented a set of self-similar solutions for two-dimensional (2D) viscous–resistive ADAFs in the presence of a dipolar magnetic field of the central accretor. They have shown that the presence of a magnetic field and its associated resistivity can considerably change the picture with regard to accretion flows.

Recent observations of hot accretion flows around active galactic nuclei indicate that they should be based on collisionless regimes.

Chandra observations provide tight constraints on both the density and temperature of gas at or near the Bondi capture radius in Sgr A* and several other nearby galactic nuclei. Tanaka & Menou (2006) have shown through calculation that the accretion discs in such systems will operate under weakly collisional conditions. Thermal conduction therefore has an important role in energy transport along the discs. The aim of this work is to consider the effects of thermal conduction, which has been largely neglected before as an energy transport mechanism, on the 2D structure of ADAFs. It could affect the global properties of hot accretion flows substantially. A few authors have considered the role of turbulent heat transport in ADAF discs (Honma 1996; Manmoto et al. 2000). Since thermal conduction acts to oppose the formation of the temperature gradient that causes it, one might expect that the temperature and density profiles for accretion flows in which thermal conduction plays a significant role are modified to appear different, compared with those flows for which thermal conduction is less effective (Shadmehri 2008).

The weak-collision nature of hot accretion flows has been addressed previously (Mahadevan & Quataert 1997). Johanson & Quataert (2007) studied the effect of electron thermal conduction on the properties of hot accretion flows under the assumption of spherical symmetry. In another interesting analysis, Tanaka & Menou (2006) studied the effect of saturated thermal conduction on optically thin ADAFs using an extension of the self-similar solution of Narayan & Yi (1994). In their solutions the thermal conduction is provided with an extra degree of freedom, which affects the global dynamical behaviour of the accretion flow. Abbassi, Ghanbari & Najjar (2008) have presented a set of self-similar solutions for ADAFs with a toroidal magnetic field in which the saturated thermal conduction has an important role in the energy transport in the radial direction. The tangled magnetic field in accretion flows would likely reduce the effective mean free path of particles. The magnitude of this reduction, which depends on the magnetic field geometry, is still unknown. We have accounted for this possibility by allowing the value of the saturated constant, ϕ_s, to vary in our solutions. The magnetic field also has an important role in transferring angular momentum along the disc. The dynamical structure of the disc will therefore be affected by the magnetic field strength and configuration. Investigating the case of a magnetized accretion flow with thermal conduction is thus an important issue.

2 THE BASIC EQUATIONS

We describe the 2D hot accretion flow in a similar manner to Narayan & Yi (1995a). We adopt spherical polar coordinates (r, θ, ϕ) for axisymmetric and steady-state flows ($\partial/\partial\phi = \partial/\partial t = 0$). The fundamental MHD governing equations can be written as follows:

the equation of continuity

$$\frac{\mathrm{D}\rho}{\mathrm{D}t} + \rho\nabla\cdot\boldsymbol{u} = 0, \tag{1}$$

the equation of motion

$$\rho\frac{\mathrm{D}\boldsymbol{u}}{\mathrm{D}t} = -\nabla\boldsymbol{P} - \rho\nabla\phi - \mu\nabla^2\boldsymbol{u} + \left(\mu_\mathrm{b} + \frac{1}{3}\mu\right)\nabla(\nabla\cdot\boldsymbol{u}) + \frac{1}{4\pi}\boldsymbol{J}\times\boldsymbol{B}, \tag{2}$$

the equation of energy

$$\rho\left[\frac{\mathrm{D}\varepsilon}{\mathrm{D}t} + P\frac{\mathrm{D}}{\mathrm{D}t}\left(\frac{1}{\rho}\right)\right] = Q_\mathrm{vis} + Q_B - Q_\mathrm{rad} + Q_\mathrm{cond}, \tag{3}$$

Gauss's law

$$\nabla\cdot\boldsymbol{B} = 0 \tag{4}$$

and the induction equation

$$\frac{\mathrm{D}B}{\mathrm{D}t} = \nabla\times(\boldsymbol{u}\times\boldsymbol{B}) + \eta\nabla^2\boldsymbol{B}, \tag{5}$$

where ρ is the density of the gas, P the pressure, ϵ the internal energy, $\boldsymbol{u}$ the flow velocity, $\boldsymbol{B}$ the the magnetic field, $\boldsymbol{J} = \nabla\times\boldsymbol{B}$ the current density, η the magnetic diffusivity, which for simplicity is assumed to be a constant parameter (see e.g. Kaburaki 2000), and μ and μ_b are the shear and bulk viscosities.

The viscous heating rate is defined as the expression

$$Q_\mathrm{vis} = 2\mu E_{ij}E^{ij} + \left(\mu_\mathrm{b} - \frac{2}{3}\mu\right)(\nabla\cdot\boldsymbol{v})^2, \tag{6}$$

where $E_{ij} = \frac{1}{2}(v_{i,j} + v_{j,i})$ is a symmetric tensor and is known as the rate-of-strain tensor.

We have adopted saturated conduction (Cowie & Mackee 1977) as

$$Q_\mathrm{cond} = -\nabla\cdot F_\mathrm{s}, \tag{7}$$

where, as we have already mentioned, $F_\mathrm{s} = 5\phi_\mathrm{s}\rho c_\mathrm{s}^3$ is the saturated conduction flux in the direction of the temperature gradient. Tanaka & Menou (2006) have shown that for very small ϕ_s their solutions coincide with the standard ADAF solutions. They have shown that by adding the saturated conduction parameter ϕ_s the effect of thermal conduction can be better seen when we approach ∼0.001–0.01. We have therefore investigated the effect of thermal conduction in this range.

Magnetic reconnection may thus lead to energy release. Also, we can consider the viscous and resistive dissipation due to a turbulence cascade. In this study, the resistive dissipation is defined as

$$Q_B = \frac{\eta}{4\pi}J^2. \tag{8}$$

On the right-hand side of the energy equation we have

$$Q_+ - Q_- + Q_\mathrm{cond} = Q_\mathrm{adv} = fQ_+ + Q_\mathrm{cond},$$

where $Q_+ = Q_\mathrm{vis} + Q_B$, $Q_- = Q_\mathrm{rad}$ and Q_adv represents the advective transport of energy and is defined as the difference between the magneto–viscous heating rate, Q_+, and the radiative cooling rate, Q_rad, plus the energy transport by conduction, Q_cond. We employ the parameter $f = 1 - (Q_-/Q_+)$ to measure the degree to which accretion flow is advection-dominated. When $f \sim 1$ the radiation can be neglected and the accretion flow is advection-dominated, while in the case of small f the disc is in the radiation-dominated

case. We can therefore rearrange the right-hand side of the energy equation to $f\mathcal{Q}_+ + \mathcal{Q}_{\rm cond}$, where $f \leq 1$. In general, it varies with r and depends on the details of the heating and cooling processes. For simplicity, it is assumed to be a constant.

For simplicity, the self-gravity of the disc and the effect of general relativity have been neglected. Also, we neglect radiation pressure in the equations because, in optically thin ADAFs, $P^{\rm gas} \gg P^{\rm rad}$. We adopt the dipolar configuration for the magnetic field. Also we have neglected the θ component of the flow velocity, $u_\theta = 0$, and the bulk viscosity of the flow, $\mu_{\rm b} = 0$. Now we formulate the basic equations (1)–(5) in spherical polar coordinates as follows:

$$\frac{\partial \rho}{\partial t} + \frac{1}{r^2}\frac{\partial}{\partial r}\left(r^2 \rho u_r\right) + \frac{1}{r}\frac{\partial}{\partial \theta}(\rho u_\theta) = 0. \tag{9}$$

The three components of the momentum equations are as follows (e.g. Mihalas & Mihalas 1984):

r component

$$\begin{aligned}\rho\left[u_r\frac{\partial u_r}{\partial r} - \frac{u_\varphi^2}{r}\right] &= -\frac{GM\rho}{r^2} - \frac{\partial p}{\partial r} + \mu\left[\frac{4}{3}\frac{\partial^2 u_r}{\partial r^2} + \frac{8}{3}\frac{1}{r}\frac{\partial u_r}{\partial r}\right.\\ &\quad \left. - \frac{8}{3}\frac{u_r}{r^2} + \frac{1}{r^2}\cot\theta\frac{\partial u_r}{\partial \theta} + \frac{1}{r^2}\frac{\partial}{\partial \theta}\left(\frac{\partial u_r}{\partial \theta}\right)\right]\\ &\quad + \frac{1}{4\pi}\left[-\frac{B_\theta}{r}\left(\frac{\partial}{\partial r}(rB_\theta) - \frac{\partial B_r}{\partial \theta}\right) - \frac{B_\varphi}{r}\frac{\partial}{\partial r}(rB_\varphi)\right],\end{aligned} \tag{10}$$

θ component

$$\begin{aligned}\rho\left[-\frac{\cot\theta}{r}u_\varphi^2\right] &= -\frac{1}{r}\frac{\partial P}{\partial \theta} + \mu\left[\frac{8}{3}\frac{1}{r^2}\frac{\partial u_r}{\partial \theta} + \frac{1}{3}\frac{1}{r}\frac{\partial^2 u_r}{\partial r \partial \theta}\right]\\ &\quad + \frac{1}{4\pi}\left[\frac{B_r}{r}\left(\frac{\partial}{\partial r}(rB_\theta) - \frac{\partial B_r}{\partial \theta}\right)\right.\\ &\quad \left. - \frac{B_\varphi}{r\sin\theta}\frac{\partial}{\partial \varphi}(B_\varphi \sin\theta)\right],\end{aligned} \tag{11}$$

φ component

$$\begin{aligned}\rho\left[u_r\frac{\partial u_\varphi}{\partial r} + \frac{u_r u_\varphi}{r}\right] &= \mu\left[\frac{\partial^2 u_\varphi}{\partial r^2} + \frac{2}{r}\frac{\partial u_\varphi}{\partial r} + \frac{1}{r^2}\cot\theta\frac{\partial u_\varphi}{\partial \theta}\right.\\ &\quad \left. + \frac{1}{r^2}\frac{\partial^2 u_\varphi}{\partial \theta^2} - \frac{u_\varphi}{r^2\sin^2\theta}\right]\\ &\quad + \frac{1}{4\pi}\left[B_\theta\left(\frac{1}{r\sin\theta}\frac{\partial}{\partial \theta}(\sin\theta B_\varphi)\right.\right.\\ &\quad \left.\left. + \frac{B_r}{r}\frac{\partial}{\partial r}(rB_\varphi)\right)\right].\end{aligned} \tag{12}$$

The equation of energy is

$$\begin{aligned}\rho\left[u_r\frac{\partial \varepsilon}{\partial r} - \frac{P u_r}{\rho^2}\frac{\partial \rho}{\partial r}\right] &= -\frac{2}{3}\mu f\left[\frac{1}{r^2}\frac{\partial}{\partial r}\left(r^2 u_r\right)\right]^2 + 2\mu f\left[\left(\frac{\partial u_r}{\partial r}\right)^2\right.\\ &\quad \left. + 2\left(\frac{u_r}{r}\right)^2 + \frac{1}{2}\left(\frac{1}{r}\frac{\partial u_r}{\partial \theta}\right)^2\right] + \frac{1}{2}\left\{r\frac{\partial}{\partial r}\left(\frac{u_r}{r}\right)\right\}^2\\ &\quad + \frac{1}{2}\left[\frac{\sin\theta}{r}\frac{\partial}{\partial \theta}\left(\frac{u_\varphi}{\sin\theta}\right)\right]^2 + \frac{\eta}{4\pi r^2}\left[\frac{\partial}{\partial r}(rB_\theta) - \frac{\partial B_r}{\partial \theta}\right]^2\\ &\quad - \frac{1}{r^2}\frac{\partial}{\partial r}\left(5\Phi_{\rm s} r^2 P^{3/2}\rho^{-1/2}\right)\\ &\quad - \frac{1}{r\sin\theta}\frac{\partial}{\partial \theta}\left(5\Phi_{\rm s}\sin\theta P^{3/2}\rho^{-1/2}\right).\end{aligned} \tag{13}$$

The three components of the induction equation are

$$u_r\frac{\partial B_r}{\partial r} = \frac{\partial}{\partial \theta}\left\{r\sin\theta\left(u_r B_\theta - \frac{\eta}{r}\left[\frac{\partial}{\partial r}(rB_\theta) - \frac{\partial B_r}{\partial \theta}\right]\right)\right\}, \tag{14}$$

$$-\frac{1}{r\sin\theta}\left(\frac{\partial}{\partial r}\left\{r\sin\theta\left[u_r B_\theta - \frac{\eta}{r}\left(\frac{\partial}{\partial r}(rB_\theta) - \frac{\partial B_r}{\partial \theta}\right)\right]\right\}\right) = 0, \tag{15}$$

$$\frac{1}{r}\left[\frac{\partial}{\partial r}(r u_\varphi B_r) + \frac{\partial}{\partial \theta}(u_\varphi B_\theta)\right] = 0. \tag{16}$$

Now we have a set of MHD equations that describes the dynamical behaviour of magnetized ADAFs. The solutions of these equations are strongly dependent on viscosity, resistivity, the degree of advection and the role of thermal conduction for the discs.

These nine partial differential equations govern non-self-gravitating, magnetized, advection-dominated viscous flows. These equations relate 15 dependent variables: $p, \rho, \epsilon, \mu, \mu_{\rm b}, \eta$ and the components of $\boldsymbol{u}$, $\boldsymbol{J}$ and $\boldsymbol{B}$. For the set of equations, we use the following standard assumptions.

The kinematic viscosity coefficient, $\nu = \mu/\rho$, is generally parametrized using the α-prescription (Shakura & Sunyev 1973),

$$\nu = \alpha c_{\rm s} H, \tag{17}$$

where $H = c_{\rm s}/\Omega_k$ is known as the vertical scaleheight, $c_{\rm s} = \sqrt{p/\rho}$ is the isothermal sound speed and the dimensionless coefficient α is assumed to be independent of r. We therefore introduce the parameter η to represent the magnetic diffusivity and insert it as a constant parameter in our equations. Both the kinematic viscosity coefficient ν and the magnetic diffusivity η have the same units and are assumed to be due to turbulence in the accretion flow. Thus it is physically reasonable to express η similarly to ν via the α-prescription of Shakura & Sunyaev (1973) as follows (Bisnovatyi-Kogan & Ruzmaikin 1976):

$$\eta = \eta_0 c_{\rm s} H. \tag{18}$$

To determine the thermodynamical properties of the flow in the energy equation, we require a constitutive relation as a function of two state variables. Therefore we choose an equation for the internal energy of $\epsilon = p/[\rho(\Gamma - 1)]$, where Γ is the ratio of specific heats of the gas.

To satisfy $\nabla \cdot \boldsymbol{B} = 0$, we may introduce a convenient functional form for the magnetic field. Owning to the axisymmetry, the magnetic field can be written as

$$\boldsymbol{B} = \boldsymbol{B}_{\rm p}(r, \theta) + B_\phi(r, \theta)\boldsymbol{e}_\phi. \tag{19}$$

Angular momentum is expected to be carried away from the disc by magnetic stresses along the externally given poloidal magnetic lines of force. In the case of a dipole-type external field it is transferred to the central accretor (Kaburaki 2000). The effect of magnetic diffusivity on magnetically driven mass accretion was studied by Kaburaki (2000). They showed that the effects of resistivity are that magnetic field lines do not rotate with the same angular speed as the disc matter and thus it suppresses the injection of magnetic helicity and magneto-centrifugal acceleration. Thus, by neglecting the toroidal component of the field, B_ϕ, we can express the poloidal component, $\boldsymbol{B}_{\rm p}$, in terms of a magnetic flux function $\Psi(r, \theta)$:

$$\boldsymbol{B} = \boldsymbol{B}_{\rm p}(r, \theta) = \frac{1}{2\pi}\nabla \times \left(\frac{\Psi}{r\sin\theta}\boldsymbol{e}_\phi\right). \tag{20}$$

It is clear that the basic equations are non-linear and we cannot solve them analytically. Therefore, it is useful to have a simple

means by which to investigate the properties of solutions. We seek a self-similar solution for the above equations. In the next section we will present self-similar solutions of these equations.

3 SELF-SIMILAR SOLUTIONS

To understand better the physical processes of our viscous–resistive ADAF accretion discs, we seek self-similar solutions of the above equations. The self-similar method is familiar from its wide applications to the full set of MHD equations. The self-similar method is not able to describe the global behaviour of accretion flows, because no boundary conditions have been taken into account. However, as long as we are not interested in the behaviour of the flow near the boundaries, such solutions are very useful.

Writing the equations in non-dimensional form, i.e. scaling all the physical variables by their typical values, brings out the non-dimensional variables. We can simply show that solutions of the following form satisfy the equations of our model:

$$\rho(r,\theta) = \rho_0\rho(\theta)(r/r_0)^{-3/2}, \tag{21}$$

$$p(r,\theta) = p_0 P(\theta)(r/r_0)^{-5/2}, \tag{22}$$

$$u_{\rm r}(r,\theta) = r\Omega_{\rm K}(r)U(\theta), \tag{23}$$

$$u_{\varphi}(r,\theta) = r\sin\theta\Omega_{\rm K}(r)\Omega(\theta), \tag{24}$$

$$B_{\rm r}(r,\theta) = \frac{B_0}{2\pi\sin\theta}\frac{d\Psi(\theta)}{d\theta}(r/r_0)^{-5/4}, \tag{25}$$

$$B_{\theta}(r,\theta) = -\frac{3B_0\Psi(\theta)}{8\pi\sin\theta}(r/r_0)^{-5/4}, \tag{26}$$

where ρ_0, p_0, B_0 and r_0 provide convenient units with which the equations can be written in non-dimensional form. Substituting the above solutions in equations (10)–(16), we obtain a set of coupled ordinary differential equations in terms of θ:

$$\frac{{\rm d}P}{{\rm d}\theta} = \frac{3\alpha P}{2(1-\alpha U)}\frac{{\rm d}U}{{\rm d}\theta} + \frac{3\rho K U}{16\pi^2\beta_0\eta_0 c_1 P\Omega^2\sin^2\theta(1-\alpha U)}\frac{{\rm d}\Omega}{{\rm d}\theta} + \frac{\rho\Omega^2\sin\theta\cos\theta}{c_1(1-\alpha U)}, \tag{27}$$

$$\frac{{\rm d}^2U}{{\rm d}^2\theta} = -\frac{2.5}{\alpha} - U - \cot\theta\frac{{\rm d}U}{{\rm d}\theta} - \frac{1}{P}\frac{{\rm d}P}{{\rm d}\theta}\frac{{\rm d}U}{{\rm d}\theta} + \frac{\rho}{c_1\alpha P}\left(1 - \frac{U^2}{2} + \Omega^2\sin^2\theta\right) + \frac{2UK\rho}{\beta_0\eta_0\alpha c_1\Omega}\left(\frac{3}{8\pi\rho\sin\theta}\right)^2, \tag{28}$$

$$\frac{{\rm d}\rho}{{\rm d}\theta} = \frac{2}{5}\frac{c_1^{-1/2}P^{-1/2}\rho^{3/2}}{\phi_{\rm s}}\left[\frac{U(3\gamma-5)}{2(\gamma-1)} - \alpha f\left\{3U^2 + \left(\frac{{\rm d}U}{{\rm d}\theta}\right)^2 + \frac{9}{4}\Omega^2\sin^2\theta + \left(\frac{{\rm d}\Omega}{{\rm d}\theta}\right)^2\sin^2\theta\right\}\right] - \frac{2}{5}\frac{f c_2\eta_0 c_1^{-5/2}P^{-5/2}\rho^{5/2}K}{16\pi^3\phi_{\rm s}\Omega}\left(\frac{3U}{4\eta_0\sin\theta}\right)^2 - 2(1-\cot\theta)\rho + 3\frac{\rho}{P}\frac{{\rm d}P}{{\rm d}\theta}, \tag{29}$$

$$\frac{{\rm d}\Omega}{{\rm d}\theta} = \frac{-A \pm \sqrt{A^2+3B}}{3}. \tag{30}$$

Finally, by definition $\beta_0 = P_0/(B_0^2/8\pi)$ and $\Omega\Psi^2 = K$, where K is an arbitrary constant, so $c_1 = (p_0/\rho_0)(GM/r_0)^{-1} = (2p_0)/(\rho_0 u_{\rm ff}^2)$ and $c_2 = (B_0^2/\rho_0)(GM/r_0)^{-1}$.

In equation (30) we have the following:

$$A = \frac{\Omega}{P}\frac{{\rm d}P}{{\rm d}\theta} + 4\Omega\cot\theta,$$

$$B = \left[\frac{9}{4} + \left(\frac{1}{\alpha} + \frac{3}{\eta_0}\right)\frac{\rho U}{c_1 P}\right]\Omega^2.$$

Equations (27)–(30) constitute a system of ordinary non-linear differential equations for the four self-similar variables Ω, P, U and ρ.

There are many techniques for solving these non-linear equations. Analytical methods can yield solutions for some simplified problems. In general, however, this approach is too restrictive and we have to use numerical methods. Here, one can employ the method of relaxation to the fluid equations (Press et al. 1992). In this method we replace ordinary differential equations by approximate finite-difference equations on a grid of points that spans the domain of interest. The relaxation method determines the solution by starting with a guess and improving it, iteratively. Based on it, this system of equations can be solved for all unknowns as a function of θ, once we are given a set of boundary conditions where constraints are placed on the flow. The boundary conditions are distributed between the equatorial plane, $\theta = \pi/2$, and the rotation axis, $\theta = 0$. We can use the Narayan & Yi (1995a,b) boundary conditions at both boundaries: the boundary conditions at $\theta = 0$ are

$$\frac{{\rm d}U}{{\rm d}\theta} = \frac{{\rm d}\Omega}{{\rm d}\theta} = \frac{{\rm d}P}{{\rm d}\theta} = \frac{{\rm d}\rho}{{\rm d}\theta} = 0, \qquad U = 0, \quad \rho = 0, \tag{31}$$

and in this method the boundary conditions at $\theta = \pi/2$ are

$$\frac{{\rm d}U}{{\rm d}\theta} = \frac{{\rm d}\Omega}{{\rm d}\theta} = \frac{{\rm d}P}{{\rm d}\theta} = \frac{{\rm d}\rho}{{\rm d}\theta} = 0. \tag{32}$$

The boundary conditions for the above equations require that variables are assumed to be regular at the endpoints. Also, the net mass accretion rate (9) provides one boundary condition for ρ:

$$\int_0^{\pi/2}\rho(\theta)U(\theta)\sin\theta\,{\rm d}\theta = -\frac{1}{2}.$$

We obtain numerical solutions for the flows with fixed values of $\eta_0 = 0.1, \Gamma = 4/3, \alpha = 0.01, 0.05, 0.1$, $f = 0.1, 0.3, 0.7$ and $\phi_{\rm s} = 0.001, 0.007, 0.01$. We consider $c_1 = 0.8$, $c_2 = 2\times10^3$ and $\beta_0 = 0.01$ (Ghanbari et al. 2007).

4 RESULTS

We have obtained numerical solutions of equations (27)–(30) for a variety of viscosity α, advection f and the thermal conduction $\phi_{\rm s}$ parameters. The three panels in Fig. 1 show the variations of various dynamical quantities in terms of polar angle θ for fixed values of viscosity and thermal conduction parameters with a sequence of increasing advection parameter f. The top panel displays the dimensionless radial velocity $U(\theta)$. $U(\theta)$ is zero at $\theta = 0$ (this is a boundary condition) and maximum at $\theta = \pi/2$. Thus, the inflow velocity reaches its maximum in the equatorial plane and vanishes along the polar axis. As expected, the velocity is sub-Keplerian. The middle panel shows the density profile $\rho(\theta)$ of the solutions. The density contrast in the equatorial and polar regions increases with a decrease in the advection parameter f. For a given α and $\phi_{\rm s}$, solutions with small values of f behave like standard thin

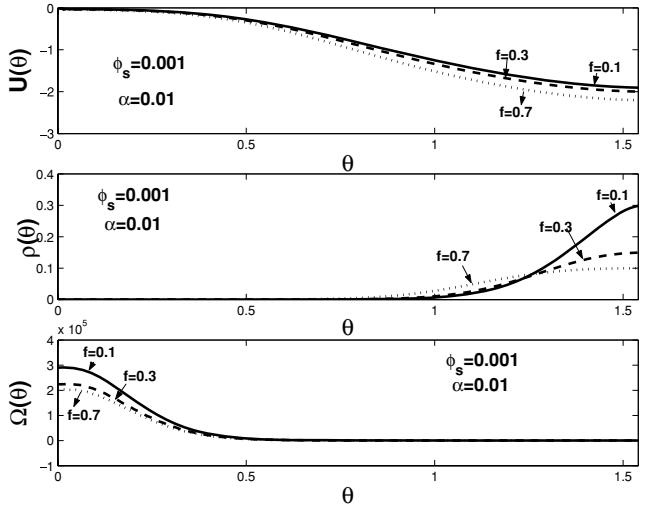

Figure 1. The self-similar solutions of radial velocity $U(\theta)$ (top), density $\rho(\theta)$ (middle) and angular velocity $\Omega(\theta)$ (bottom) as a function of polar angle θ corresponding to $\Gamma = 4/3, \eta_0 = 0.1, \beta_0 = 0.01$ and $f = 0.1, 0.3, 0.7$ for $\alpha = 0.01$ and $\phi_s = 0.001$.

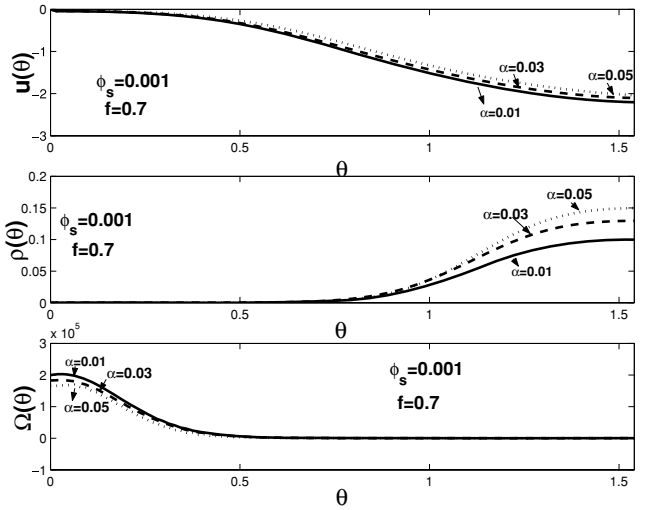

Figure 2. The self-similar solutions of radial velocity $U(\theta)$ (top), density $\rho(\theta)$ (middle) and angular velocity $\Omega(\theta)$ (bottom) as a function of polar angle θ corresponding to $\Gamma = 4/3, \eta_0 = 0.1, \beta_0 = 0.01$ and $\alpha = 0.01, 0.03, 0.05$ for $f = 0.7$ and $\phi_s = 0.001$.

discs; as might be expected, these solutions correspond to $f \to 0$ and so a small fraction of energy would be advected. In the opposite advection-dominated limit, $f \to 1$, our solutions describe nearly spherical flows which rotate with velocities far below the Keplerian. The bottom panel shows the profile of the angular velocity $\Omega(\theta)$. $\Omega(\theta)$ decreases with increases in the advection in the accretion discs. We find that in the inner boundary $U(\theta)$ is essentially independent of advection parameter f, but at intermediate values of θ the radial velocity is modified by f; in Shadmehri's (2004) solutions, two distinct regions in the $U(\theta)$ profile could be recognized. The bulk of accretion occurs from the equatorial plane at $\theta = \pi/2$ to $\theta = \theta_s$, where the radial velocity is zero. In the Narayan & Yi solutions there is no zero inflow at $0 < \theta < \pi/2$. Our solutions show that at any given θ the radial velocity is non-zero, and when we increase the advection parameter the radial velocity will be increased.

Here we may comment on the fact that when the advection parameter, f, tends to zero, our disc does not correspond to a globally cooling flow because of the appearance of a thermal conduction term in the energy transport equation. When f tends to 1 our discs are not fully advective, because some part of the energy generated by viscosity will be transported by thermal conduction.

Fig. 2 displays the behaviour of the radial and angular velocities and density profile for different values of the viscosity parameter, for fixed advection and thermal conduction parameters. We find that the value of the viscous parameter, α, quantitatively (but not qualitatively) affects the dynamical variables of the accretion flow. For a larger value of the viscous parameter, the radial inflow decreases and the density would be increased overall, which is compatible with the results presented by Ghanbari et al. (2007).

The panels in Fig. 3 show, for fixed advection and viscosity parameters with a sequence of thermal conduction parameters, (1) the radial velocity increases with an increase in the thermal conduction parameter, (2) the density profile increases with a decrease in the thermal conduction parameter and (3) the angular velocity decreases with an increase in ϕ_s in the accretion discs.

In Fig. 4 we display the isodensity contours in the meridional plane. The top, middle and bottom panels display the isodensity

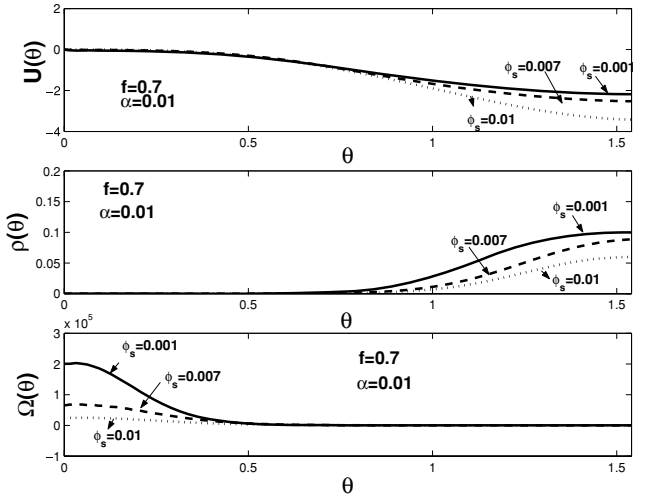

Figure 3. The self-similar solutions of radial velocity $U(\theta)$ (top), density $\rho(\theta)$ (middle) and angular velocity $\Omega(\theta)$ (bottom) as a function of polar angle θ corresponding to $\Gamma = 4/3, \eta_0 = 0.1, \beta_0 = 0.01$ and $\phi_s = 0.001, 0.007, 0.01$ for $f = 0.7$ and $\alpha = 0.01$.

profiles for different values of conduction, advection and viscous parameters, respectively. The panels in Fig. 4 show that the disc seems to be thick. Solutions with the same f but different values of α are distinguishable from one another. By adding a viscous parameter the geometrical shape of the disc becomes more and more thick. These advection-dominated solutions have very similar properties to the approximated solution derived by Narayan & Yi (1994), Ghanbari et al. (2007) and Shadmehri (2004).

The overall structure of the dynamical variables remains very close to the original two-dimensional ADAF solutions of Narayan & Yi (1995a,b). This solution is denser close to the equator than at the pole, and it is something like a 'thin disc' surrounded by a hot coronal atmosphere.

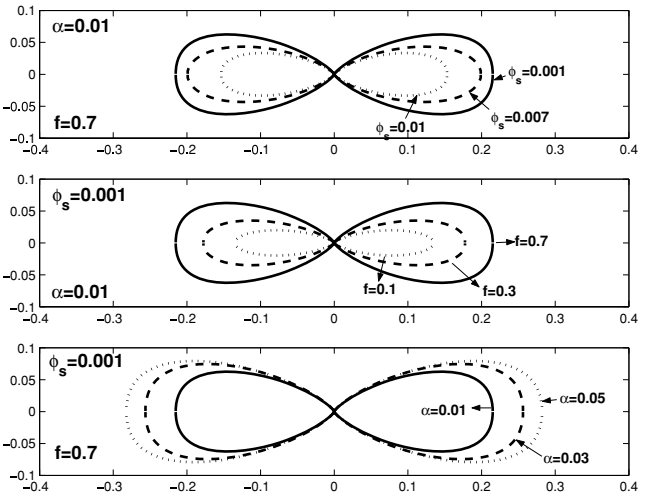

Figure 4. Isodensity contours for $\Gamma = 4/3, \eta_0 = 0.1, \beta_0 = 0.01$ and $\phi_s = 0.001, 0.007, 0.01$ for $f = 0.7, \alpha = 0.01$ (top), $f = 0.1, 0.3, 0.7$ for $\alpha = 0.01, \phi_s = 0.001$ (middle) and $\alpha = 0.01, 0.03, 0.05$ for $f = 0.7, \phi_s = 0.001$ (bottom).

As the values of ϕ_s are increased, the solutions start to deviate substantially from the standard solutions, with faster radial flow and slower rotation (i.e. becoming more pressure-supported) at the equator. By increasing ϕ_s, the density reduces in the equatorial plane, and the density profile becomes more uniform. It gradually approaches spherical symmetry. This behaviour of the solutions is shared by the original ADAF solutions and Ghanbari et al.'s (2007) work.

5 SUMMARY AND CONCLUSION

The main aim of this investigation was to obtain an axisymmetric self-similar advection-dominated solution for viscous–resistive accretion flow with a poloidal magnetic field in the presence of thermal conduction. Using the basic equations of fluid dynamics in spherical polar coordinates (r, θ, φ), we have found the self-similar solutions for thick discs to derive a set of coupled differential equations that govern the dynamics of the system. We have then solved the equations using the relaxation method, by considering boundary conditions and using the α-prescription (Shakura & Sunyaev 1973) in order to extract some of the similarity functions in terms of the polar angle θ.

We showed that the radial and rotational velocities are well below the Keplerian velocity. The bulk of accretion with nearly constant velocity occurs in the regions that extend from the equatorial plane to a given θ, which strongly depends on the advection parameter f. In a non-advective regime (low f) we have a standard thin accretion disc, but for high f the accretion is nearly spherical.

It is difficult to evaluate the precise picture of radiatively inefficient accretion flow in the presence of thermal conduction with a self-similar method. However, this method can reproduce the overall dynamical structure of the discs with a set of given physical parameters. Even though conduction heats up the accretion flows locally, the reduced density resulting from the larger inflow velocity leads to a net decrease in the expected level of free–free emission. The very steep dependence of synchrotron emission on the electron temperature (e.g. Mahadevan & Quataert 1997) suggests that hotter solutions (with conduction) may be more efficient radiatively (Tanaka & Menou 2006). From self-similar solutions alone, we can determine how the global structure of the flow can be affected by thermal conduction. For small enough values of ϕ_s the solutions remain very close to the Ghanbari et al. (2007) solutions. The main difference between their solution and the standard solution of 2D ADAFs of Narayan & Yi (1995a) is the presence of a dipolar magnetic field and its corresponding resistivity. In our case, we add extra physics by adding the thermal conduction as a mechanism for energy transport. By adding the thermal conduction, the solution starts deviating substantially from the original ADAFs, with faster radial inflow at the equator. These results well agree with Tanaka & Menou (2006).

The presence of a magnetic field with a poloidal configuration will affect the role of thermal conduction. Compared with the non-magnetic field solution (Tanaka & Menou 2006), in our case the existence of magnetic resistivity can produce more energy to be advected. The B-field configuration can also affect the energy transportation along accretion discs. However, the main aim of this work is to study a quasi-spherical magnetized flow directly by solving the relevant MHD equations. Although we have made some simplifications in order to treat the problem analytically, our self-similar solutions show that the input parameters, such as thermal conduction and viscous parameters, the magnetic field and its resistivity can really change the typical behaviour of the physical quantities of ADAF discs. Of course, our self-similar solutions are too simple to make any comparison with observations. However, we think that one may relax the self-similarity assumptions and solve the equations of the model numerically. This kind of similarity solution could greatly facilitate testing and interpretation of the results.

ACKNOWLEDGMENTS

We are grateful to the referee for a very careful reading of the manuscript and for suggestions that have helped us to improve the presentation of our results.

REFERENCES

Abbassi S., Ghanbari J., Najjar S., 2008, MNRAS, 388, 663
Abramowicz M. A., Czerny B., Lasota J. P., Szuszkiewicz E., 1988, ApJ, 332, 646
Abramowicz M. A., Chen X., Kato S., Lasota J. P., Regev O., 1995, ApJ, 438, L37
Bisnovatyi-Kogan G. S., Ruzmaikin A. A., 1976, Ap&SS, 42, 401
Chen X., 1995, MNRAS, 275, 641
Cowie L. L., Mackee C. F., 1977, ApJ, 275, 641
Ghanbari J., Salehi F., Abbassi S., 2007, MNRAS, 381, 159
Hameury J. M., Lasota J. P., Maclintock J. E., Narayan R., 1997, ApJ, 489, 234
Honma F., 1996, PASJ, 48, 77
Ichimaru S., 1977, ApJ, 214, 840
Igumenshchev I., Abramowicz M., Narayan R., 2000, ApJ, 537, L27
Johanson B. M., Quataert E., 2007, ApJ, 660, 1273
Kaburaki O., 2000, ApJ, 531, 210
Lasota J. P., Abramowicz M. A., Chen X., Krolik J., Narayan R., Yi I., 1996, ApJ, 462, 142
Mahadevan R., Quataert E., 1997, ApJ, 490, 605
Manmoto T., Kato S., Nakamura K., Narayan R., 2000, ApJ, 529, 127
Mihalas D., Mihalas B. W., 1984, Foundation of Radiation Hydrodynamics. Oxford Univ. Press, New York
Narayan R., Yi I., 1994, ApJ, 428, L13

Narayan R., Yi I., 1995a, ApJ, 444, 238
Narayan R., Yi I., 1995b, ApJ, 452, 710
Narayan R., Maclintock J. E., Yi I., 1996, ApJ, 457, 821
Narayan R., Igumenshchev I. V., Abramowicz M. A., 2000, ApJ, 539, 798
Press W. H., Teukolsky S. A., Vetterling W. T., Flannery B. P., 1992, Numerical Recipes. Cambridge Univ. Press, Cambridge
Shadmehri M., 2004, A&A, 424, 379
Shadmehri M., 2008, Ap&SS, 317, 201
Shakura N. I., Sunyev R. A., 1973, A&A, 24, 337
Shapiro S. L., Lightman A. P., Eardley D. M., 1976, ApJ, 204, 187
Tanaka T., Menou K., 2006, ApJ, 649, 345

This paper has been typeset from a TEX/LATEX file prepared by the author.